Failure of the mean-field approach in the out-of-equilibrium Anderson model

B. Horváth,[1] B. Lazarovits,[1,2] O. Sauret,[1] and G. Zaránd[1]

[1]*Theoretical Physics Department, Institute of Physics, Budapest University of Technology and Economics, Budafoki út 8, H-1521 Budapest, Hungary*

[2]*Research Institute for Solid State Physics and Optics, Hungarian Academy of Sciences, Konkoly-Thege M. út 29-33, H-1121 Budapest, Hungary*

(Received 4 December 2007; published 31 March 2008)

To explore the limitations of the mean-field approximation, frequently used in *ab initio* molecular electronics calculations, we study an out-of-equilibrium Anderson impurity model in a scattering formalism. We find regions in the parameter space where both magnetic and nonmagnetic solutions are stable. We also observe a hysteresis in the nonequilibrium magnetization and current as a function of the applied bias voltage. The mean-field method also predicts incorrectly local moment formation for large biases and a spin polarized current, and unphysical kinks appear in various physical quantities. The mean-field approximation thus fails in every region where it predicts local moment formation.

DOI: 10.1103/PhysRevB.77.113108 PACS number(s): 73.63.Kv, 75.20.Hr, 71.23.An, 73.23.−b

The Anderson impurity model[1] (AIM) has been the subject of great theoretical and experimental interest in the past decades (for a review, see Ref. 2). There is a number of experimental systems including quantum dots, or single atoms and molecules contacted by leads, which provide experimental realizations of various versions of the AIM under out-of-equilibrium conditions. These systems are not just prototypes of out-of-equilibrium systems but a theoretical understanding of them would be crucial for future molecular electronics and mesoscopic applications.

Anderson constructed his famous model in Ref. 1 to describe local moment formation and solved it within the mean-field (MF) approximation. Within this approximation, he found a phase transition to a state where magnetic moments are formed. Further work revealed that, in reality, quantum fluctuations of this local moment lead to the formation of a Kondo singlet between the impurity and conduction electrons[2] at low temperature, where the impurity spin is thus completely screened. The spontaneous symmetry breaking found by Anderson is thus an artifact of the mean-field approximation. Nevertheless, the MF treatment indicates clearly the regions of strong correlations, and it can also serve as a starting point for accurate approximations as in the local moment approach[3] or interpolative perturbation theory[4,5] (IPT). The latter approach can easily be generalized to nonequilibrium situations[6,7] using the Keldysh formalism.[8]

In lack of more accurate methods, the mean-field approximation is also used in molecular electronics calculations, where local density approximation or eventually the Hartree–Fock equations are solved in a scattering state or in the Keldysh approach to describe moment formation.[9] However, it is not clear at all how reliable these approximations are. The purpose of this Brief Report is to shed some light on the weaknesses of the nonequilibrium mean-field approach on the simplest possible test case, the out-of-equilibrium Anderson model, and to show where usual *ab initio* calculations should fail. Our conclusion is that the mean-field approach fails qualitatively and quantitatively essentially everywhere where it predicts local moment formation. Our study, which is based on the scattering state formalism, is complementary to the recent work of Komnik and Gogolin,[10] who used Green's function formalism to study the mean-field equations of the nonequilibrium Anderson model. As we shall see, in the strongly correlated regions, several artifacts emerge such as nonequilibrium driven spontaneous symmetry breaking as well as multiple stable solutions which lead to the appearance of hysteresis. These instabilities are probably also parts of the reasons why nonequilibrium IPT suffers from all kinds of instabilities. These instabilities were avoided in previous works by applying spin-independent approximations[11] or using an interpolative self-energy[4] or both.[12]

The nonequilibrium AIM Hamiltonian consists of four parts. The first part describes a single impurity level with energy ε_d and an on-site Coulomb interaction (U),

$$H_d = \sum_{\sigma=\uparrow,\downarrow} \varepsilon_d d_\sigma^\dagger d_\sigma + U n_\uparrow n_\downarrow, \tag{1}$$

where $d_\sigma^\dagger$ and d_σ are the creation and annihilation operators of the impurity electrons corresponding to spin state σ and $n_\sigma = d_\sigma^\dagger d_\sigma$. The second and third terms describe the left (L) and right (R) leads which we model by tight-binding chains,

$$H_\alpha = \sum_{k,\sigma} (-2\tilde{t}\cos k + \mu_\alpha) c_{k\alpha\sigma}^\dagger c_{k\alpha\sigma}. \tag{2}$$

Here, $\alpha \in (L,R)$, $c_{k\alpha\sigma}^\dagger$ and $c_{k\alpha\sigma}$ are the creation and annihilation operators of a conduction electron of wave number $k \in \{0,\pi\}$ in lead α, $\tilde{t}$ is the hopping along the leads, and μ_α is the chemical potential of the left or the right lead. The chemical potentials of the two leads are different due to a finite bias voltage leading to a nonequilibrium situation. The fourth part, H_t, describes the tunneling between the leads and the impurity,

$$H_t = \sum_\sigma [d_\sigma^\dagger (V_- c_{-1\sigma} + V_+ c_{1\sigma}) + \text{H.c.}]. \tag{3}$$

Here, $V_\mp$ are the hybridization matrix elements between the impurity and the left and the right leads, and $c_{l=\pm1\sigma}$ denote the conduction electron annihilation operators on the sites next to the impurity; sites along the left and right chains are labeled by $l=\{-\infty,\ldots,-1\}$ and $l=\{1,\ldots,\infty\}$, respectively.

 ©2008 The American Physical Society

For the sake of simplicity, here we study a symmetrical situation, $V_-=V_+=V$, but our conclusions are rather independent of this assumption.

To study the Hamiltonian above, we used a mean-field approximation and replaced the impurity term as

$$H_d \to H_d^{MF} = \sum_\sigma (\varepsilon_d + U\langle n_{-\sigma}\rangle) d_\sigma^\dagger d_\sigma. \tag{4}$$

The nonequilibrium expectation value of the occupation numbers $\langle n_\sigma\rangle$ in Eq. (4) can be obtained by solving self-consistent equations as will be discussed later. The expression $\varepsilon_d + U\langle n_{-\sigma}\rangle$ can be regarded as an effective energy level of spin-σ electron. The hybridization between impurity and conduction electrons gives rise to a finite lifetime for impurity states, reflected in the broadening of the effective impurity levels with a finite width, $\Gamma = 2\pi V^2 \rho_0 = V^2/\tilde{t}$, where ρ_0 is the density of states (DOS) of the conduction electrons at the Fermi level of the half-filled leads.

To evaluate the nonequilibrium expectation values, $\langle n_\sigma\rangle$, we shall use a scattering formalism. The annihilation operator of the left-coming scattering state of energy ε and spin σ can be expressed as

$$c_\sigma(\varepsilon) = \sum_{l<0} c_{l\sigma} e^{ikR_l} + \alpha_\sigma(\varepsilon) \sum_{l<0} c_{l\sigma} e^{-ikR_l} + \beta_\sigma(\varepsilon) \sum_{l>0} c_{l\sigma} e^{ik'R_l} + \gamma_\sigma(\varepsilon) d_\sigma. \tag{5}$$

Here, $c_{l\sigma}$ is the annihilation operator of the lth site and $\alpha_\sigma(\varepsilon)$, $\beta_\sigma(\varepsilon)$, and $\gamma_\sigma(\varepsilon)$ are the reflection, transmission, and dot coefficients, respectively, which we obtain by solving the corresponding Schrödinger equation. Since the energy is conserved in course of the scattering process, the wave numbers k and k' are connected by the dispersion relation $\varepsilon = -2\tilde{t}\cos k + \mu_L = -2\tilde{t}\cos k' + \mu_R$. Waves coming from the right hand side can be constructed in a similar way. The occupation numbers are then calculated from the dot coefficients, $\gamma_\sigma(\varepsilon)$ and $\gamma'_\sigma(\varepsilon)$ corresponding to the states coming from the left and the right, respectively,

$$\langle n_\sigma\rangle = \rho_0 \int_{-\infty}^{\infty} d\varepsilon [|\gamma_\sigma(\varepsilon)|^2 f_L(\varepsilon) + |\gamma'_\sigma(\varepsilon)|^2 f_R(\varepsilon)], \tag{6}$$

where the DOS of leads is approximated by its value at Fermi level and $f_\alpha(\varepsilon) \equiv f(\varepsilon - \mu_\alpha)$ is the Fermi function.

In the large bandwidth approximation ($\tilde{t}\to\infty$, $\Gamma = V^2/\tilde{t}$ finite), the occupation numbers become

$$\langle n_\sigma\rangle = \frac{\Gamma}{2\pi} \int_{-\infty}^{\infty} \frac{f_L(\varepsilon) + f_R(\varepsilon)}{(\varepsilon - \varepsilon_d - U\langle n_{-\sigma}\rangle)^2 + \Gamma^2} d\varepsilon, \tag{7}$$

which simplifies further for zero temperature as

$$\langle n_\sigma\rangle = \sum_{\alpha\in(L,R)} \frac{1}{2\pi} \cot^{-1}\left(\frac{\varepsilon_d + U\langle n_{-\sigma}\rangle - \mu_\alpha}{\Gamma}\right). \tag{8}$$

These self-consistent equations can also be obtained using the Keldysh formalism.[10] Equation (7) or (8) is solved iteratively by assuming that the applied bias is symmetrical, $\mu_L = \mu/2$ and $\mu_R = -\mu/2$. In these calculations, the bias voltage is increased or decreased gradually and the local stability of the solutions is always checked.

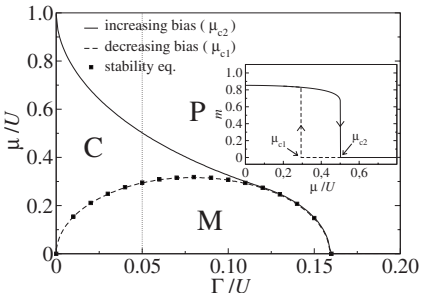

FIG. 1. Magnetic (M), coexistence (C), and paramagnetic (P) regions as a function of μ/U and Γ/U values for $\varepsilon_d/U = -1/2$. The boundaries of the regions obtained by increasing and decreasing bias are plotted with solid and dashed lines, respectively. The exactly evaluated boundary curve is indicated by squares. Inset: magnetization as a function of increasing and decreasing bias voltages for $\Gamma/U = 0.05$ (along the dotted line in the main figure).

First, let us discuss the bias dependence of the occupation numbers at $T=0$. In the inset of Fig. 1, the magnetization $m = \langle n_\uparrow\rangle - \langle n_\downarrow\rangle$ is plotted both for increasing and decreasing bias voltages at a fixed ratio of $\Gamma/U = 0.05$ for the symmetric Anderson model ($\varepsilon_d/U = -0.5$). In equilibrium, at zero bias, the impurity possesses a finite magnetic moment for the chosen parameter set, while in case of high bias voltages ($\mu > 0.5$), the stable solution is paramagnetic. Between the two limiting cases, a region appears, $\mu_{c1} < \mu < \mu_{c2}$, where both the magnetic and the nonmagnetic solutions are stable. We shall refer to this region as a coexistence region. The existence of multiple stable solutions for the occupation numbers in this region is reflected in the hysteresis of the magnetization too. The sharp decay of the magnetization shown in the inset of Fig. 1 and the existence of a hysteresis between the critical fields indicate clearly a first order transition, predicted incorrectly by the MF solution.

The parameter space can thus be divided into magnetic (M), paramagnetic (P), and coexistence (C) regions. In the paramagnetic regions, a single stable solution exists only ($\langle n_\uparrow\rangle = \langle n_\downarrow\rangle$), while in the magnetic one, two stable magnetic (corresponding to magnetizations $\pm m$) and one unstable paramagnetic solutions can be found. In the coexistence region, two magnetic and one paramagnetic stable solutions and two unstable magnetic solutions exist. Therefore, these regions can be distinguished by the number of the solutions of Eq. (8). In the symmetric case, when $\langle n_\uparrow\rangle + \langle n_\downarrow\rangle = 1$, the easiest way to construct a "phase diagram" is to sweep possible values of $\langle n_\uparrow\rangle - \langle n_\downarrow\rangle$ pairs, substitute them into Eq. (8), and count the number of solutions for different parameter sets.

In the paramagnetic region, one can exploit the fact that Eq. (8) has a nonmagnetic solution for every possible parameter set. Therefore, one can substitute $\langle n_\uparrow\rangle = \langle n_\downarrow\rangle$ into Eq. (8) and search only for nonmagnetic states. The region of stability for this solution can then be determined through a linear stability analysis.[10,13]

Figure 1 shows a typical magnetic "phase diagram" as a function of μ/U and Γ/U for the symmetric nonequilibrium

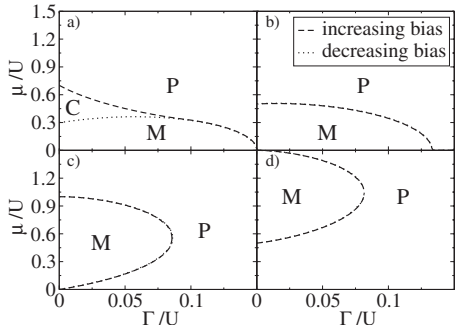

FIG. 2. "Phase diagrams" as a function of μ/U and Γ/U for $T=0$ and different ε_d values: $\varepsilon_d/U=$ (a) −0.35, (b) −0.25, (c) 0, and (d) 0.25. Notations of the regions are the same as in Fig. 1. The increasing and decreasing bias voltages are denoted by dashed and dotted lines, respectively.

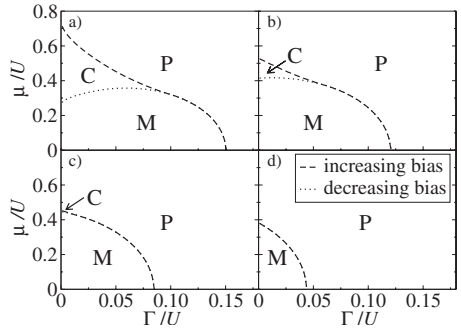

FIG. 3. "Phase diagrams" as a function of μ/U and Γ/U for $\varepsilon_d/U=-0.5$. The temperature $T/U=$ (a) 0.051, (b) 0.101, (c) 0.151, and (d) 0.201. Notations of the regions are the same as in Fig. 1. The increasing and decreasing bias voltages are denoted by dashed and dotted lines, respectively.

AIM at $T=0$. At the "upper critical line" μ_{c2}, the magnetic solution becomes unstable. In the magnetic case, the effective levels corresponding to different spins are not equally occupied and lie at different energies. The magnetic solution becomes unstable when the value of the bias voltage reaches approximately the effective energy of one of the two differently occupied levels.

The critical line μ_{c1} in Fig. 1 marks, on the other hand, the border of stable paramagnetic solutions. In the special case, $\varepsilon_d=-U/2$, the two spin occupations are $\langle n_{\uparrow,\downarrow}\rangle=0.5$ in the whole paramagnetic region, and the magnetic boundary equation simplifies to $\mu^2+16\Gamma^2-8U\Gamma/\pi=0$. This analytical result is nicely reproduced by our numerical stability analysis (see Fig. 1).

The values of μ_{c1} and μ_{c2} are functions of Γ/U and ε_d/U; for increasing Γ/U, the coexistence and magnetic regions disappear and only the nonmagnetic solution survives. In Fig. 2, the "phase diagrams" can be seen as a function of μ/U and Γ/U at $T=0$. Depending on the value of ε_d, we can distinguish four different regions: *empty regime* ($\varepsilon_d>0$), *mixed valence regime* ($\varepsilon_d\approx 0$), *local moment regime* ($-U\leqslant\varepsilon_d\leqslant 0$), and a *doubly occupied regime* ($\varepsilon_d<-U$) which behaves similarly to the empty regime by particle-hole symmetry.

In the local moment regime, shown in Figs. 1 and 2(a), for $\varepsilon_d\approx -U/2$, there is approximately one electron on the impurity forming a local spin moment. In equilibrium, this finite magnetic moment is predicted on the dot below a critical value of Γ/U, and this moment is destroyed by a large enough bias voltage. The coexistence region only appears in this local moment regime and vanishes above $\varepsilon_d\approx -U/4$ [see Fig. 2(b)].

In the empty regime ($\varepsilon_d\geqslant 0$), shown in Figs. 2(c) and 2(d), the equilibrium magnetization completely disappears. However, surprisingly, the MF solution predicts the appearance of local moments for small Γ and $2\varepsilon_d\leqslant\mu\leqslant 2\varepsilon_d+U$ biases. This intriguing local moment formation has a simple physical meaning: For large values of U/Γ and $2\varepsilon_d\leqslant\mu\leqslant 2\varepsilon_d+U$, the bias voltages are large enough to inject an electron to the empty level; however, they are not large enough to overcome the Coulomb energy of injecting a second electron to the local level. Therefore, electrons pass through the dot one by one, and a fluctuating magnetic moment appears on the dot. Note that in this regime, the magnetization is induced exclusively by the finite bias voltage.

The overall effect of the temperature in the applied MF approximation is to destroy the magnetic moment on the impurity and drive the system to be paramagnetic. Figure 3 shows the temperature dependence of the "phase diagram" in the symmetric case. The coexistence region gradually vanishes for increasing temperatures, while the magnetic and paramagnetic regions get larger. Increasing the temperatures further, the magnetic region disappears too.

The previous results are summarized in Fig. 4 for a fixed ratio $\Gamma/U=0.05$ that is already sufficiently small to find the coexistence and magnetic regions in the local moment regime. The whole "phase diagram" is symmetric to $\varepsilon_d/U=-0.5$ due to the electron-hole symmetry. Note that the coexistence region only exists close to the electron-hole symmetric point, $\varepsilon_d/U\approx -0.5$. For large asymmetries (double or zero equilibrium occupation), a nonequilibrium magnetic solution appears, while in equilibrium, only the paramagnetic solution exists. This magnetic region has also been observed although not discussed in detail in Ref. 10.

The mean-field solution also leads to the appearance of nonphysical features in the transport properties of the impurity. We calculated the transport properties within the MF approximation using the Landauer-Büttiker formalism[14] but similar results can be obtained applying the Keldysh formalism.[13] The current can be evaluated as

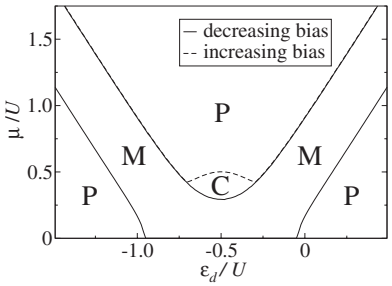

FIG. 4. Magnetic (M), coexistence (C), and paramagnetic (P) regions as a function of μ/U and ε_d/U values for $\Gamma/U=0.05$.

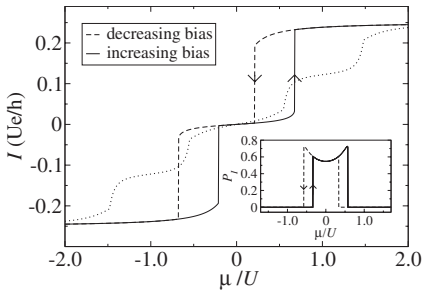

FIG. 5. The current as a function of the bias voltage for $\varepsilon_d/U=-0.5$ (solid and dashed lines) and $\varepsilon_d/U=0.25$ (dotted line) for $\Gamma/U=0.02$. Hysteresis can be observed in the current in the local moment regime. Inset: the polarization of the current for $\varepsilon_d/U=-0.35$ and $\Gamma/U=0.02$.

$$I_\sigma \equiv \frac{e}{h}\int_{-\infty}^{\infty} d\varepsilon [f_L(\varepsilon)-f_R(\varepsilon)]|t_\sigma(\varepsilon)|^2. \tag{9}$$

Here, the transmission coefficient $t_\sigma=\beta_\sigma\sqrt{v_{k'}/v_k}$ is normalized to the flux, with v_k and $v_{k'}$ the velocities of incident and transmitted electrons with wave numbers k and k'. Applying the large bandwidth approximation again, the current can be written for finite temperatures as

$$I_\sigma = \frac{e}{2\pi\hbar}\int_{-\infty}^{\infty} d\varepsilon \frac{\Gamma^2[f_L(\varepsilon)-f_R(\varepsilon)]}{(\varepsilon-\varepsilon_d-U\langle n_{-\sigma}\rangle)^2+\Gamma^2}, \tag{10}$$

with $\langle n_\sigma\rangle$ the nonequilibrium occupation numbers obtained from Eq. (7). This integral can be trivially evaluated at $T=0$ temperature.

Figure 5 shows the current as a function of bias for two different level positions in the strongly correlated regime. For $\varepsilon_d/U=-0.5$, we find hysteresis in the current. For $\varepsilon_d/U=0.25$, on the other hand, no hysteresis appears but the current shows a two-step behavior as a function of bias voltage. In this empty regime, the MF equations thus account qualitatively correctly for the charging of the local level, but the kinks appearing in the $I(\mu/U)$ curve are due to the incorrectly predicted symmetry breaking and are thus again artifacts of the MF solution.

In the inset of Fig. 5, we have plotted the polarization of the current, $P_I \equiv (I_\uparrow - I_\downarrow)/(I_\uparrow + I_\downarrow)$, as a function of μ. In the symmetric case, the current is not polarized due to the electron-hole symmetry, but for small electron-hole asymmetries, a hysteresis appears in the polarization too. In general, the polarization is finite whenever a local moment appears on the impurity, and there is no electron-hole symmetry.

To conclude, we have studied the out-of-equilibrium Anderson model in the framework of the scattering formalism combined with a mean-field approximation. This method, frequently used in molecular transport calculations, incorrectly predicts a magnetic phase transition as well as a bias-induced magnetic moment formation, accompanied by hysteresis in various physical quantities and the coexistence of multiple solutions. The MF approach thus fails whenever correlations become important. These artifacts of the mean-field approach should alert physicists who study transport through strongly correlated and magnetic molecules and urge one to use more sophisticated methods that avoid spontaneous symmetry breaking and account for dynamical effects.

ACKNOWLEDGMENTS

We are grateful to László Szunyogh for valuable discussions and remarks. This research has been supported by Hungarian Grants No. OTKA NF061726, T046303, and F68726.

[1] P. W. Anderson, Phys. Rev. **124**, 41 (1961).
[2] A. C. Hewson, in *The Kondo Problem to Heavy Fermions* (Cambridge University Press, Cambridge, England, 1993).
[3] D. E. Logan, M. P. Eastwood, and M. A. Tusch, J. Phys.: Condens. Matter **10**, 2673 (1998).
[4] A. Martín-Rodero, M. Baldo, F. Flores, and R. Pucci, Solid State Commun. **44**, 911 (1982).
[5] A. A. Aligia and L. A. Salguero, Phys. Rev. B **70**, 075307 (2004).
[6] A. L. Yeyati, A. Martín-Rodero, and F. Flores, Phys. Rev. Lett. **71**, 2991 (1993).
[7] A. A. Aligia, Phys. Rev. B **74**, 155125 (2006).
[8] J. Rammer and H. Smith, Rev. Mod. Phys. **58**, 323 (1986).
[9] D. Waldron, L. Liu, and H. Guo, Nanotechnology **18**, 424026 (2007), and references therein; D. Waldron, P. Haney, B. Larade, A. MacDonald, and H. Guo, Phys. Rev. Lett. **96**, 166804 (2006); K. Palotás, B. Lazarovits, L. Szunyogh, and P. Weinberger, Phys. Rev. B **70**, 134421 (2004).
[10] A. Komnik and A. O. Gogolin, Phys. Rev. B **69**, 153102 (2004).
[11] B. Horvatic, D. Sokcevic, and V. Zlatic, Phys. Rev. B **36**, 675 (1987).
[12] H. Kajueter and G. Kotliar, Phys. Rev. Lett. **77**, 131 (1996).
[13] B. Horváth, Diploma thesis, Budapest University of Technology and Economics, 2006.
[14] M. Büttiker, Y. Imry, R. Landauer, and S. Pinhas, Phys. Rev. B **31**, 6207 (1985).